Asian Journal of Nanoscience and Materials 3 (2020) 93-102

Asian Journal of Nanoscience and Materials

Journal homepage: www.ajnanomat.com

Original Research Article

Electrochemical reduction of CO_2 using cuprous oxide particles supported on carbon paper substrate

Fahd Sikandar Khan[a,*], Masakazu Sugiyama[a], Katsushi Fujii[b], Yoshiaki Nakano[c]

[a] *Department of Advance Interdisciplinary Studies, School of Engineering, University of Tokyo, Japan*

[b] *Nakamura Laboratory, Research Cluster for Innovation, RIKEN, 2-1 Hirosawa, Wako, Saitama, 351-0198, Japan*

[c] *Department of Electrical Engineering, School of Engineering, University of Tokyo, Japan*

ARTICLE INFORMATION

Received: 27 July 2019
Received in revised: 23 August 2019
Accepted: 30 August 2019
Available online: 27 November 2019

DOI: 10.26655/AJNANOMAT.2020.2.1

KEYWORDS

CO_2 reduction
Electrocatalysis
Cuprous oxide
Ethylene
Formic acid

ABSTRACT

Electrochemical reduction of CO_2 is so important in mitigating the greenhouse related environmental concerns. Recently, oxidized forms of metals instead of pure metals have gained a great deal of attention due to the difference in product selection between the two classes of electrode materials. Since copper has been widely used in producing carbon-intensive products, various studies have been dedicated to evaluate its oxidized form. In this research study, we focused on using cuprous oxide particles supported on hydrophobic carbon paper substrate. The structure of the carbon paper provides unique reaction sites while the micron-sized particles can help to provide new insight about using smaller surface area to volume ratio as compared to previous reports on oxidized copper nanoparticles. Formic acid, ethylene, and CO were produced as a result of our experiments which show improved product selection compared with the pure copper nanoparticles. The potential and time dependence of these products are presented in this study along with a discussion on the origin of CO_2 reduction.

Corresponding author, email: fahdskhan@yahoo.com (F. Sikandar Khan).
Tel.: +819017021608.

Graphical Abstract

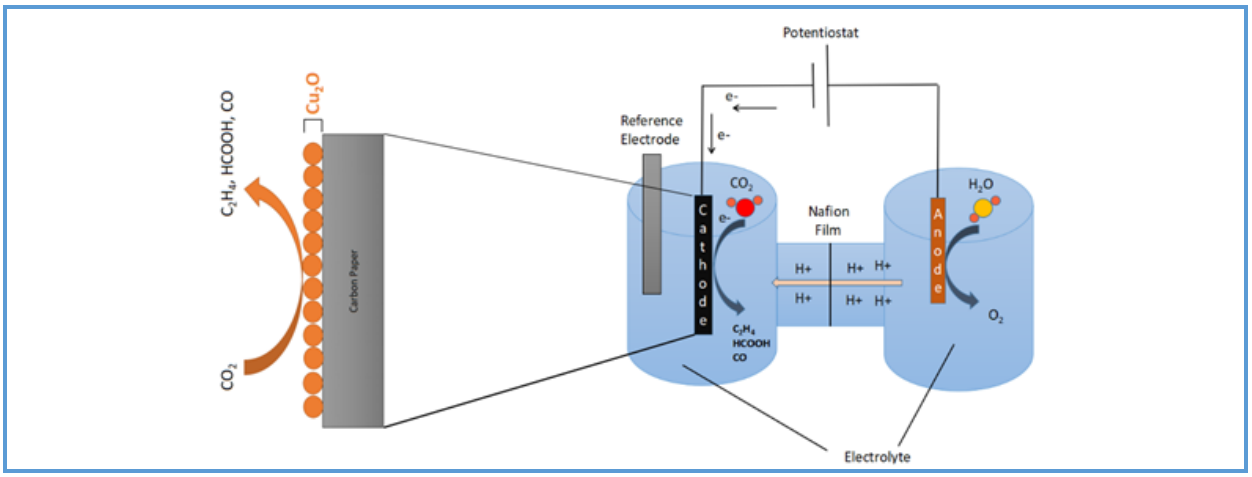

Introduction

Renewable energy sources such as solar and wind have started to play an increasing role in the energy landscape of our planet. However, a major drawback of these sources has been the intermittent supply and lack of energy stability. Research about the scenarios for sustainable energy suggest that the electrochemical reduction of CO_2 (CO_2RR) can help to address this issue by utilizing the excess energy from renewable energy sources by converting CO_2 into some chemical compounds such as methane, methanol or carbon monoxide (for Syngas), which can serve as energy vectors and can be used to compensate the energy fluctuations from the renewable energy sources [1].

To date, most of the studies on CO_2 reduction have focused on metal electrodes in which copper [2, 3] has been the most popular due to its propensity for producing higher order carbon products. Recently, metal-oxide catalysts have begun to gain attention as well due to their decent faradaic efficiency and selectivity for electrochemical reduction of CO_2. Metal oxides have also shown difference in product distribution compared to pure metals [4].

Among metal oxides, cuprous oxide (Cu_2O) has proven to be the most active one for generating multi-carbon products [5–7]. The first such study on Cu_2O was reported by *Frese* et al. in 1991 [8] who had compared results between air-oxidized and anodized copper and had observed methanol as the major product. *Le* et al. [9] in 2011 had also studied oxidized copper (Cu_2O) and had reported production of methanol along with traces of CO while the following year *Li et al.* [10] used thicker layers of anodized Cu and decreased the onset potentials for CO formation.

More lately, efforts are being made towards improving the selectivity of multi-carbon products by changing the morphology and sizes of Cu_2O particles. *Wang* et al. [11] in 2019 was able to improve the efficiency towards ethylene (C_2H_4) by using Cu_2O catalysts grown on graphite sheets functionalized with ionic liquid. CH_4, C_2H_6, and other products were also reported in the study. Similarly in 2019, *Tan* et al. [12] developed a novel metal organic framework in Cu_2O-based electrodes and reported improved faradaic efficiency towards CH_4 while also producing other higher order carbon products.

The role between oxide layer and metal phase and their contribution towards product selectivity in CO_2RR has also been an issue of debate [13, 14]. It was demonstrated by *Kim* et al. [14] that electrodeposited Cu_2O can aid in the selective formation of C_2H_4 over CH_4 and had concluded that both the oxide component and metal affect the selective electroreduction of CO_2 toward multi-carbon products. Previous works have shown that the product selectivity of Cu_2O is dependent upon the morphology and size of the oxide particles while the formation of Cu^0 with O vacancies within these Cu_2O particles during CO_2RR is also considered as an important factor in the efficacy of Cu_2O as catalysts [15, 16]. *Wang* et al. [11] had suggested that the oxide matrix plays a key role in maintaining high performance of oxide-derived Cu^0 and that the grain boundaries impact the product selectivity during CO_2RR.

In this study, we report the use of micron-sized cuprous oxide (Cu_2O) particles to analyze the impact of using smaller area to volume ratio on product selectivity. Carbon fiber paper (CP) was chosen as the substrate material due to its hydrophobic composite of carbon and carbon fibers which apart from being conductive also allow higher porosity and cheaper price compared with that of the glassy carbon substrates while offering enhanced structural rigidity than carbon cloth. The surface porosity in electrode structures has been reported to change both reagent and product transport pathways [17] and these changes in transport phenomena have shown to increase current density and change product selectivity [18, 19]. Since most studies have used smaller sizes of Cu_2O particles in combination with either copper metal [20–23] or glassy carbon [12, 24], it was our hypothesis that the use of larger size of Cu_2O particles supported on a structurally porous CP substrate would offer new product distributions.

Experimental

Materials and Methods

The Cu_2O powder was commercially procured from Sigma Aldrich vendor. The method of preparation for this powder was based on chemical reduction approach which typically involves the reduction of metal salts in various solvents and agents, which allows micron-size particles to form [25–29]. Cu_2O particles were deposited on a commercially-procured fuel cell carbon paper (TPI-120T). A solution was prepared with ethanol as the solvent and nafion as the adhesive material along with the Cu_2O particles in the ratio 30:5:1, respectively. The mixed solution was treated ultrasonically for 30 min to form a homogeneous ink. A 50 µL solution was then drop-casted onto 1 cm^2 of carbon paper (CP), which acted as a substrate. The control electrodes in the experiments were CP without the Cu_2O particles.

Home-made H-type leak-tight electrochemical cells were used for CO_2 reduction, with 100 cm^3 volume and 70 mL of electrolyte. The end-products were collected for further analysis. The working and reference electrodes were put in the same compartment and separated from the counter electrode by a nafion film (DuPont: N117). Ag/AgCl reference electrode was employed while a platinum electrode was used as the counter electrode. A working device for the reduction of CO_2 requires a source of protons and electrons and so platinum was used for the oxygen evolution reaction (OER), which served as the other half-reaction for this purpose. Water was oxidized as: $2\ H_2O \rightarrow 4\ H^+ + 4\ e^- + O_2$. 0.5 M $KHCO_3$ with a pH of 8.59 was used in the cathode and anode electrolyte. The pH changed to 7 after CO_2 purging for 25 min prior to the experiment while the pH changes during the experiment were not observed. Since CO_2 reduction is a

redox reaction, evolution of O_2 takes place at the counter electrode and so the separation between the working and counter electrodes helps to ensure that the recombination of the products produced on these two electrodes can be effectively prohibited. The gas product was then sampled manually through syringe using HP 6890 Gas Chromatographer (GC). The liquid phase products were determined by Ion Chromatography (IC) and collected with a Thermo Scientific Dionex ICS-5000 system. The Panalytical X'Pert X-ray diffraction machine was used to study the different peaks originating from the substrate and Cu_2O. Hitachi SU8020 high resolution scanning electron microscope with EDX analysis was used for characterization while Hitachi Miniscope TM-1000 was used for images of CP substrate. Electrochemical experiments were performed using Solartron 1280C potentiostat while a stir bar was used within the electrochemical cell. Electrodes were prepared by affixing a copper wire on one side of the CP substrate with kapton tape, which was then covered with aryldyte to ensure that there was no interaction between the electrolyte and the copper wire. The electrolyte was purged with CO_2 or Ar for 25 min prior to experimental or control trials, respectively. All experiments were conducted in ambient conditions.

Results and Discussion

A loading amount of 1 and 2 mg/cm^2 was tested for CO_2 electrochemical reduction. SEM/EDX analysis determined the particle size distribution of Cu_2O to be between 2 µm and 5.5 µm. The relatively large size of Cu_2O grains in our study allowed for a different surface area and orientation from the previously reported studies. The SEM image of CP in Figure 1 and Cu_2O on CP (Figure 2) distinguishes between the structure of the substrate and electrode with catalyst loading of 2 mg/cm^2.

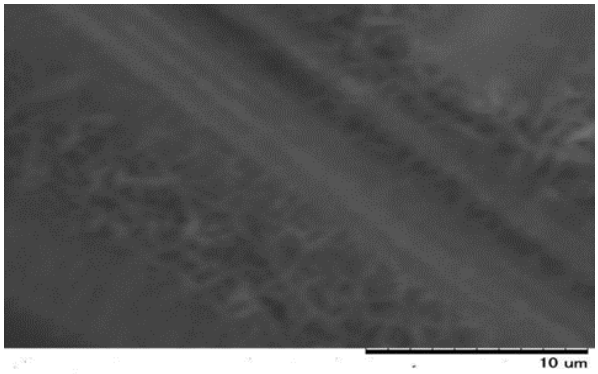

Figure 1. SEM images of carbon paper substrate

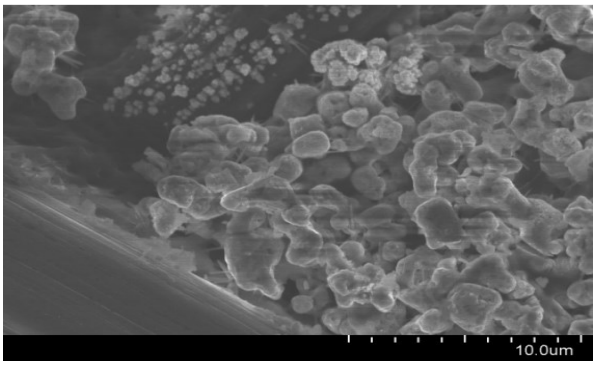

Figure 2. SEM images of Cu_2O deposited substrate

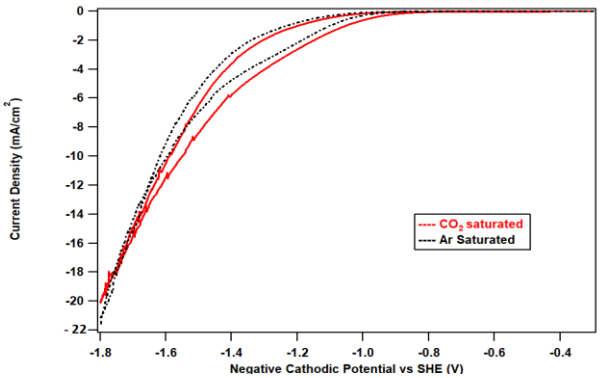

Figure 3. IV response of Cu_2O particles in CO_2-saturated (solid red line) and Ar-saturated (dotted black line) electrolytes

The relative IV response in CO_2 saturated and inert environment (Figure 3) revealed a nominal difference in current densities, reflecting that hydrogen evolution reaction (HER) takes place in the inert environment. In the CO_2-saturated environment, on the other hand, HER competes with CO_2RR. A stirrer at

350 rpm had been employed to ensure that the bubble formation did not impact the current densities. It is pertinent to mention that even if all other conditions are constant, the absence of stirrer in an EC setup can drastically change the IV response. As an example, for loading amount of 1 mg/cm^2, it was reported by *Chang* et al. [30] that the current density for Cu_2O on carbon cloth with no stirring, was 6 mA/cm^2 at -1.7 V *vs* SCE. However, we observed current densities of almost 11 mA/cm^2 with a stirrer at around the same potential and loading. Experiments conducted without a stirrer at exactly the same conditions gave us a current density of about 7 mA/cm^2.

The electrochemical reduction of CO_2 using Cu_2O particles with loading amount of 2 mg/cm^2 produced formic acid as the major product. Ethylene and carbon monoxide were produced as the secondary products. The faradaic efficiency of these products varied with the cathodic potential and are shown in Figure 4**a**. A base-10 log scale is used for the y-axis to better represent the trend between FE and cathodic potential. The experiments were conducted for 35 min. The ethylene presence was detected from the onset of CO_2 reduction at -1300 mV *vs* SHE. The FE for ethylene was 2.8% at the onset potential, which decreased to almost 0.7% at -1600 mV *vs* SHE, and then went up again to 5.9% at a potential of 1800 mV *vs* SHE. The faradaic efficiency for CO followed a similar trend to C_2H_4, whereby its FE decreased at potentials of -1500 mV and -1600 mV but increased to almost 5.1% at -1800 mV. The formic acid however showed an opposite trend with a FE of 13.3% at -1300 mV, which reached upto 31% at -1600 mV and then decreased to about 8.8% at -1800 mV.

This inverse trend between faradaic efficiency of formic acid and C_2H_4, CO can possibly reflect different origins of CO_2RR. Control electrodes (carbon paper) generated

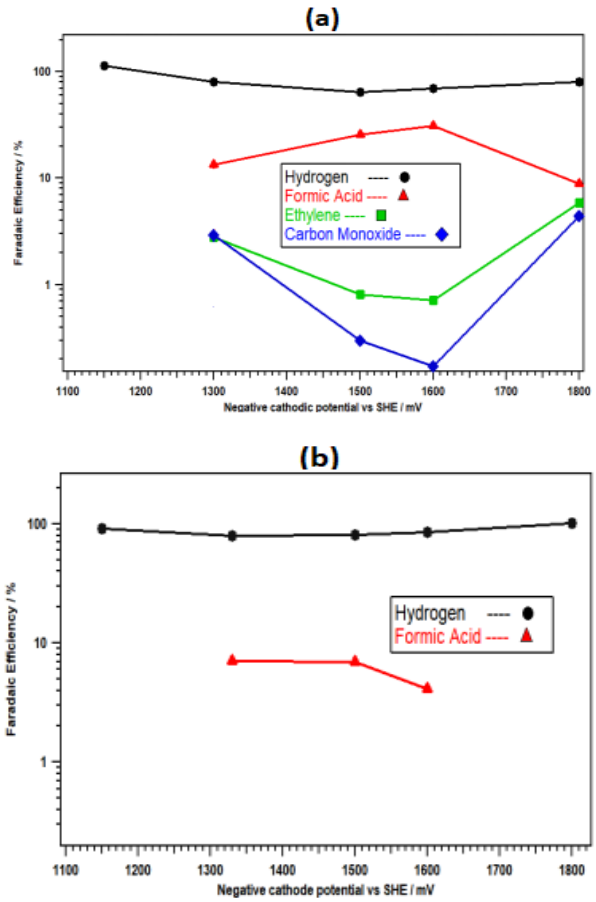

Figure 4. Faradaic Efficiency (base-10 log) against negative cathodic potential for a) Cu_2O samples with 2 mg/cm^2 loading b) control samples (CP without Cu_2O)

formic acid during CO_2RR (Figure 4**b**) but the maximum faradaic efficiency was only 7% at -1300 mV *vs* SHE. However, the faradaic efficiency of the formic acid was significantly increased when cuprous oxide particles were employed. It can be observed that at potentials of -1500 and -1600 mV *vs* SHE, the Cu_2O catalysts aid in enhancing the faradaic yields of the primary product (formic acid) being produced on the CP substrate during CO_2RR. For potentials outside this range, Cu-based catalyst played a more active role in formation of the CO and C_2H_4. It has been reported that CO formation on Cu_2O aids in suppressing HER [31] and increases conversion of hydrocarbon products since CO acts an as intermediate

specie [32] for higher order carbon products. This is the reason why CO and C_2H_4 followed a similar trend in which the increase of CO lead to an increase of C_2H_4 while a decrease in CO led to a decrease in C_2H_4. Interestingly, methane and methanol were not detected.

For the experiments conducted at potentials more negative than -1800 mV *vs* SHE, the current density increased to more than 20 mA/cm^2, causing slight color degradation of the electrodes, which may be a reflection of Cu_2O erosion. Increased nafion binder ratio during the electrode preparation can possibly help to maintain electrode stability [33]. Electrodes with Cu_2O loading of 2 mg/cm^2 were experimented for multiple time duration of 35 min, 60 min, 90 min and 120 min at -1300 mV *vs* SHE and -1600 mV *vs* SHE and this time dependence of the products is shown in Figure 5. A subtle trend could be observed for both potentials: a gradual decrease of FE for formic acid was observed while C_2H_4 especially at -1300mV *vs* SHE slightly increased with time. This can originate from the thermodynamic reducibility of the Cu_2O phase under CO_2 reduction conditions, which has been a major concern for attempts to use the Cu oxidation state to control selectivity for CO_2 reaction products [22]. The purboix diagram for Cu in aqueous solutions [34] indicates that Cu^0 is more stable at negative potentials *vs* SHE at neutral pH. From the results presented here, it can be speculated that at least a partial reduction of the Cu_2O component has been taking place with time which impacts the product selectivity during CO_2RR. Since energy level calculations have shown that it is the reduction of the bulk phase which is more likely than surface reduction of Cu_2O grains [35, 36], it can be speculated that the surface layer may exist as a hybrid structure made up of oxidized Cu at the interface with H_2O molecules, along with a neighboring Cu^0 component beneath.

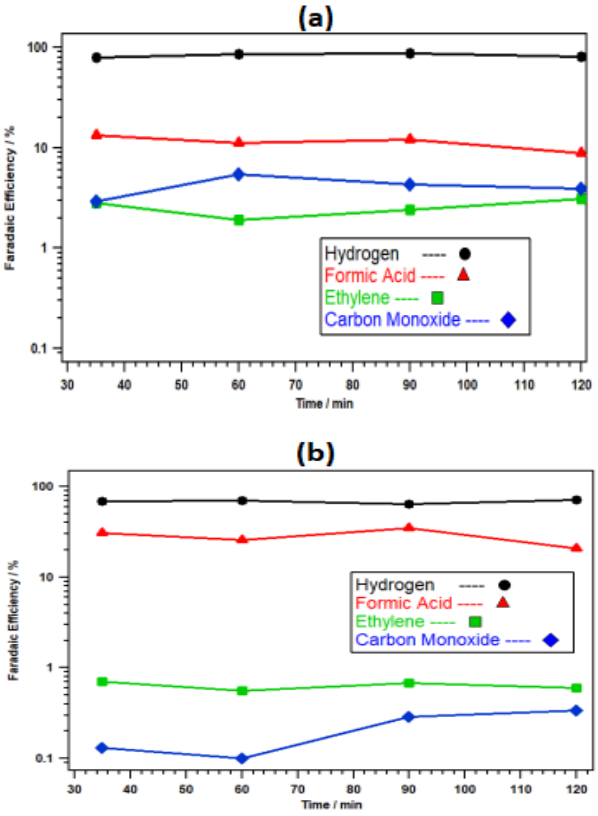

Figure 5. Time dependent faradaic efficiency for Cu_2O samples at a) -1300 mV *vs* SHE b) -1600 mV *vs* SHE. A base-10 log scale is used in y-axis to better visually represent the FE for products below 1%

To analyze the impact of loading amount of catalyst on the trend originating from the Cu_2O/CP, 1 mg/cm^2 of Cu_2O was tested for CO_2RR and the faradaic results are shown in Figure 6. Formic acid continued to remain the dominant product from CO_2RR and the maximum faradaic yield of 13% was seen at -1500 mV. In comparison with the control electrode (carbon paper), the FE towards formic acid was still almost twice greater. Lower loading of catalysts show that product selectivity is affected by the competing H_2 reaction on the carbon paper and the sizable diminishing of Cu_2O active sites is suggested to decrease the overall activity for CO_2RR. C_2H_4 faradaic efficiency remained around 1% for the entire potential range. Our experiments with

0.5 mg/cm² loading did not provide consistent reproducability while increasing the loading amount to 4 mg/cm² also did not significantly impact the product distribution and so their results are not discussed here.

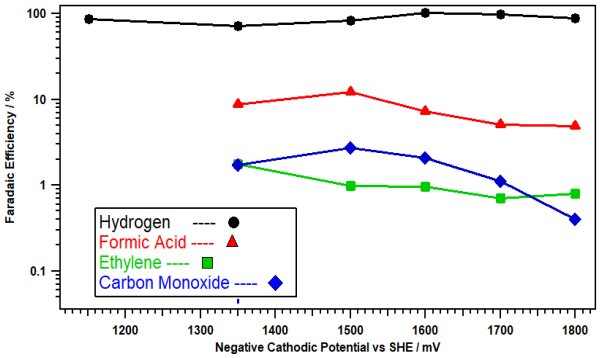

Figure 6. Faradaic Efficiency (base-10 log) against negative cathodic potential for Cu_2O samples with 1 mg/cm² loading

Energy dispersive X-ray (EDX) spectroscopy was used to analyze the elemental composition of cuprous oxide electrode for loading amount of 2 mg/cm² and is shown in Table 1. The Cu/O ratio was approximately 1.5 due to the higher presence of Cu in the Cu_2O structure. The possibility of substrate oxidization and margin of error in EDX measurement may be the reason for the deviation from the expected Cu/O ratio of 2. Carbon was detected from the substrate while potassium presence was a result of the reduction of K+ ions [11] present in the electrolyte. Fluorine was detected due to the hydrophobic polymers on CP that assist in suppressing the CO_2RR activity on CP.

The XRD data of our electrode in Figure 7 shows only Cu_2O and carbon peaks before and after CO_2RR. The peak positions are at a good agreement with those for Cu_2O powder obtained from the International Center of Diffraction Data card (JCPDS file no. 05-0667), confirming the formation of a single cubic phase Cu_2O with a cuprite structure [37], where the oxygen atoms form a body centred cubic lattice while copper atoms form a face-centred cubic lattice such that every copper atom is half-way between two oxygen atoms. The peaks with 2θ values of 29.6, 36.5, 42.4, 61.5, 73.6 and 77.6 correspond to the crystal planes of 110, 111, 200, 220, 311 and 222 of crystalline Cu_2O, respectively. Peaks originating from the substrate CP were observed at 2θ value of 26.5 and 54.6 [38]. No characteristic peaks of Cu metal or CuO were observed in the XRD patterns for samples measured after CO_2RR. An in-situ raman spectroscopy study by Mandal *et. al.* [39] for the electrochemical reduction of CO_2 on Cu_2O, had reported that the reduced Cu phase in Cu_2O can easily and instantaneously undergo re-oxidation after CO_2RR experiments which may explain the absence of any Cu phase in our XRD measurements.

Table 1. Elemental analysis of Cu_2O/CP electrode after CO_2RR experiments

Element	Atomic %
Copper	11.44
Oxygen	7.50
Carbon	69.58
Fluorine	10.83
Potassium	0.64
	100.00

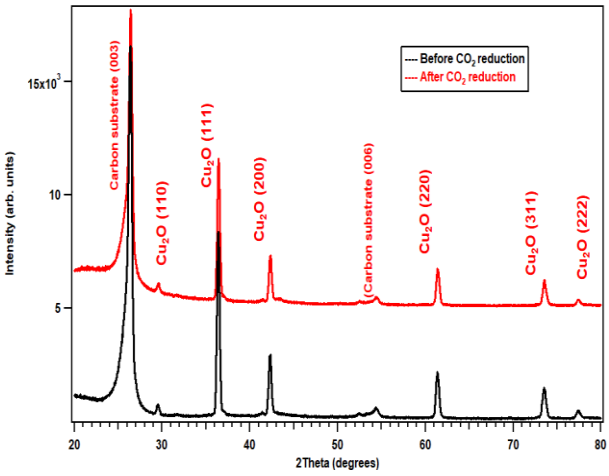

Figure 7. Cu_2O XRD peaks before (black) and after (red) CO_2RR

The production of formic acid during the CO_2RR experiments is suggested to originate from the difference in binding energy for the intermediate species. CO production occurs primarily through a key carbon-bound intermediate, *COOH, while formic production proceeds through a key oxygen-bound intermediate, *OCHO [40]. Since formic acid was also observed from experiments involving control electrodes (CP), it reflects that the surface of carbon paper has a propensity towards *OCHO and the presence of Cu-based catalysts assist in enhancing the faradaic yields of formic acid. The modification of reaction energy for formic acid generation due to Cu has been previously reported in DFT studies of *Peterson* [41] and *Shin* [42].

The selectivity towards C_2H_4 instead of CH_4 is also an important observation. *Hori* et al. [43] had previously compared a series of different orientations of single crystal Cu and had shown that C_2H_4 formation was strongest on Cu (711) surfaces while *Baturina* et al. [44] and *Riske* et al. [45] had also suggested that C2 products are produced during CO_2RR on low-coordination sites and low-index facets (edges, defects, and corners) due to their similarity to Cu (311), Cu (511), and Cu (711). We believe that the partial reduction of Cu_2O particles and the oxygen vacancies has an impact on the grain boundaries [14–16] and allow formation of low coordination surface sites which cause preferential production of C_2H_4. A factor in the performance of Cu_2O during CO_2 electrolysis is believed to originate from the hydroxide ions (OH^-) that are generated during CO_2RR at the electrode surface. The rise of local pH close to the surface layer has been reported to limit the reduction of Cu_2O to metallic Cu at the electrolyte interface, which assists in the continuous generation of C_2H_4 [46].

In summary, this study demonstrates selectivity towards C2 ethylene with no CH_4 presence. It is our contention that the use of particles with smaller area to volume ratio was able to allow a Cu_2O structure, wherein the reduced Cu^0 with oxygen vacant sites had an impact on the grain boundaries and allowed selective production of C_2H_4 from among the possible multi-carbon products. CO, which is an intermediate specie for C_2H_4, was also observed. Formic acid production is believed to have originated from the CP substrate, while the presence of Cu-based catalysts caused a potential dependent enhancement of its faradaic efficiency. The production of formic acid as liquid product is also more important due to its higher relative profitability index; a term defined by the ratio of economic value to the required amount of electrical energy per mole of products [47].

Conclusions

The electrochemical reduction of CO_2 was attempted on the Cu_2O particles with loading amounts of 1 mg/cm^2 and 2 mg/cm^2. Electrochemical reduction of CO_2 showed that formic acid was the major product along with C_2H_4 and CO while hydrogen gas was the parasitic product from the experiments. The use of these catalysts with relatively bigger size on a hydrophobic carbon paper substrate helped to narrow the selectivity of the products in comparison with the copper metal, which generally produced more number of products during CO_2RR. We contend that this work can inspire to further study micron-sized cuprous oxide catalysts for achieving similar selectivity with higher faradaic efficiency of C2 products from CO_2RR.

Disclosure Statement

No potential conflict of interest was reported by the authors.

References

[1]. Kumar B., Brian J., Atla V., Kumari S., Bertram K., White R., Spurgeon J. *Catal. Today*, 2016, **270**:19

[2]. Hori Y., *Modern Aspects of Electrochemistry*, Springer, New York, 2008, pg 89

[3]. Kuhl K., Cave E., Abram D., Jaramillo T. *Energy Environ Sci*., 2008, **5**:7050

[4]. Luna P.D., Quintero-Bermudez R., Dinh C., Ross M.B., Bushuyev O.S.,Todorovic P., Regier T., Kelley S., Yang P., Sargent E. *Nat. Catal*., 2018, **1**:103

[5]. Lee C.W., Yang K.D., Nam D.H., Jang J.H., Cho N.H., Im S.W., Nam K.T. *Adv. Mater*., 2018, **30**:1704717

[6]. Chen C., Sun X., Lu L., Yang D., Ma J., Zhu Q., Qian Q., Han B. *Green Chem*., 2018, **20**:4579

[7]. Seunghwa L., Dahee K., and Jaeyoung L., *Angew. Chem. Int. Ed*., 2015, **54**:14701

[8]. Frese K.W. *Journal of Electrochemical Society*, 1991, **138**:3338

[9]. Le M., Ren M., Zhang Z., Sprunger P. T., Kurtz R. L., Flake J.C. *Journal of the Electrochemical Society*, 2011, **158**:45

[10]. Li C.W., Kanan M.W. *Journal of the American Chemical Society*, 2012, **134**:7231

[11]. Wang W., Ning H., Yang Z., Feng Z., Wang J., Wang X., Mao Q., Wu W., Zhao Q., Hu H., Song Y., Wu M. *Electrochimica Acta*, 2019, **306**:360

[12]. Tan X., Yu C., Zhao C., Huang H., Yao X., Han X., Guo W., Cui S., Huang H., Qiu J. *ACS Appl. Mater. Interfaces*, 2019, **11**:9904

[13]. Lee S., Ocon J. D., Son Y., Lee J. *J. Phys. Chem. C*., 2015, **119**:4884

[14]. Kim D., Lee S., Ocon J. D., Jeong B., Lee J. K., Lee J., *Phys. Chem. Chem. Phys*., 2015, **17**:824

[15]. Lum Y., Ager J.W. *Angew. Chem. Int. Ed*., 2018, **57**:551

[16]. Eilert A., Cavalca F., Roberts F.S., Osterwalder J., Liu C., Favaro M., Crumlin E.J., Ogasawara H., Friebel D., Pettersson L.G., Nilsson A. *J. Phys. Chem. Lett.*, 2018, **8**:285

[17]. Burdyny T., Smith W.A. *Energy Environ. Sci*., 2019, **12**:1442

[18]. Kas R., Kortlever R., de Wit P., Milbrat A., Luiten-Olieman M., Benes N., Koper M., Mul G. *Nature Communications*, 2016, **7**:10748

[19]. Hana X., Wang M., Linh M., Bedford N., Woehl T., Thoi S. *Electrochimica Acta*, 2019, **297**:545

[20]. Lee S., Kim D., Lee J. *Angew. Chem. Int. Ed. Engl.,* 2015, **54**:14701

[21]. Ren D., Ang BS-H., Yeo B.S. *ACS Catalysis*, 2016, **6**:8239

[22]. Li C.W., Ciston J., Kanan M.W. *Nature*, 2014, **508**:504

[23]. Kim D., Kley C.S., Li Y., Yang P. *PNAS*., 2017, **114**:10560.

[24]. Ning H., Mao Q., Wang W, Yang Z., Wang X., Zhao Q., Song Y., Wu M. *Journal of Alloys and Compounds*, 2019, **785**:7

[25]. Dang T., Le, T, Blanc E.F, Dang M. *Adv. Nat. Sci. Nanosci. Nanotechnol*., 2011, **2**:15009

[26]. John W., Ayi A., Chinyere A., Providence A., Bassey I. *Advanced Journal of Chemistry-Section A.*, 2019, **2**:175

[27]. Gomaa E., Abdel H., Mahmoud M., El Kot D. *Adv. J. Chem. A*., 2019, **2**:1

[28]. Ayesha K., Audi R., Rafia Y., Ren C. *Int. Nano Lett*., 2016, **6**:21

[29]. Sachin S., Ashok B., Chandrashekhar M. *J. Nano Electron. Phys*., 2016, **8**:01035

[30]. Chang T., Liang R., Wu P. Chen J.Y., Hsieh Y.C. *Material Letters*, 2009, **63**:1001

[31]. Hori Y., Murata A., Takahashi R., Suzuki S. *Chem. Let*t., 1987, **16**:1665

[32]. Hori Y., Murata A., Takahashi R. *J. Chem. Soc*., *Faraday Trans*., 1989, **85**:2309

[33]. Bugayonga J., Griffin G.L. *ECS Trans*., 2013, **588**:81

[34]. Wanatabe M., Shibata M., Kato A., Azuma M., Sakata T. *J. Electrochem. Soc*., 1991, **138**:3382

[35]. Kim J.Y., Rodriguez J.A., Hanson J.C., Frenkel A.I., Lee P. *J. Am. Chem. Soc*., 2003, **125**:10684
[36]. Maimaiti Y., Nolan M., Elliott S. *Phys. Chem. Chem. Phys.,* 2014, **16**:3036
[37]. Kooti M., Matouri L. *Transaction F: Nanotechnology*, 2010, **17**:73
[38]. Zhang X., Lu X., Shen Y., Han J., Yuan L., Gong L., Xu Z., Bai X., Wei M., Tong Y., Gao Y., Chen J., Zhou J., Wang L.Z. *Chem. Commun*., 2011, **47**:5804
[39]. Mandal L., Yang K.R., Motapothulav M.R,. Ren D., Lobaccaro P., Patra A., Sherburne M., Batista V.S., Yeo B.S., Ager J.W., Martin J. *Venkatesan T. ACS Appl. Mater. Interfaces*, 2018, **10**:8574
[40]. Jeremy T., Chuan S., Etosha R., Toru H., David N., Kendra P., Christopher H., Nørskov J., Jaramillo T. *ACS Catal*., 2017, **7**:4822
[41]. Peterson A.A., Abild-Pedersen F., StudtF., Rossmeisl J., Nørskov J. *Energy Environ. Sc*i. 2010, **3**:1311
[42]. Shin H.S., Song J.Y., Jiang Y., *Mater. Lett*. 2009, **63**:39
[43]. Hori Y., Takahashi I., Koga O, Hoshi N. *Journal of Physical Chemistry*, 2002, **106**:15
[44]. Baturina O., Lu Q., Padilla M., Le X., Li W., Serov A., Artyushkova K., Atanassov P., Xu F., Epshteyn A., Brintlinger T., Schuette M., Collins G. *ACS Catal*., 2014, **4**:3682
[45]. Reske R., Mistry H., Behafarid F., Cuenya B.R., Strasser P. *J. Am. Chem. Soc*., 2014, **136**:6978
[46]. Ko C., Lee W. *Surf. Interface Anal*., 2010, **42**:1128
[47]. Meenesh R., Singha L., Clarka, B., Bella A. *PNAS*, 2015, **112**:6111

How to cite this manuscript: Fahd Sikandar Khan*, Masakazu Sugiyama, Katsushi Fujii, Yoshiaki Nakano. Electrochemical reduction of CO_2 using cuprous oxide particles supported on carbon paper substrate. *Asian Journal of Nanoscience and Materials*, 3(2) 2020, 93-102. DOI: 10.26655/AJNANOMAT.2020.2.1